Bubble "Lightning" Streamers from Laser Induced Cavities in Phosphoric Acid

Juan M. Rosselló[1,2], Dwayne S. Stephens[1], Robert Mettin[1]

[1] *Drittes Phys. Inst., Georg-August-Universität, 37077 Göttingen, Germany. Email: robert.mettin@phys.uni-goettingen.de*

[2] *Institut für Physik, Otto-von-Guericke-Universität, 39106 Magdeburg, Germany, Email: jrossello.research@gmail.com*

Introduction

The dynamics of acoustic cavitation bubble structures relies on complicated interactions of the sound field with the oscillating and moving gas voids, and on mutual interaction of the bubbles [1]. Once nucleated, a bubble is subject to acoustic forces: the primary Bjerknes force $\vec{F}_{Bj}$ arising from the oscillating pressure gradients of the incident sound field [2, 3], and the secondary Bjerknes force $\vec{F}^{(2)}_{Bj}$ which results from the gradients in sound scattered from neighboring bubbles [4, 5]. Both lead to the observed bubble structure and pattern formation, which still is not completely understood due to its complexity. To better explore such dynamics, a targeted nucleation of bubbles can serve as an important tool, in particular for transient phenomena that otherwise occur only via spontaneous nucleation. Here we report on the laser pulse seeding of a line-like bubble ensemble in phosphoric acid and the subsequent dynamics of emerging bubble streamers, which give the impression of lightnings. The observations are favourably compared to a series of numerical simulations, leading to the conclusion that multibubble cluster motion can be described to some extent by particle models with individual bubbles.

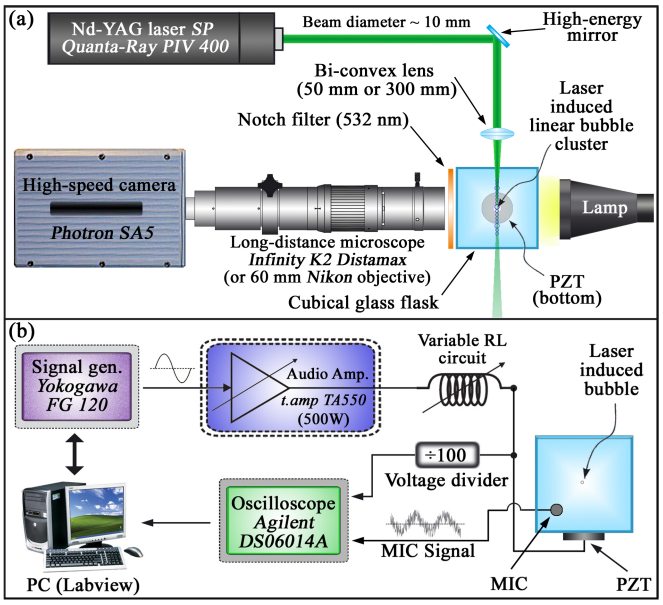

Figure 1: Experimental setup: (a) Laser bubble seeding and imaging arrangements. (b) Acoustic driving system. Reprinted from J. M. Rosselló et al., Physics of Fluids, 30, 122004, (2018), with the permission of AIP Publishing.

Experimental setup

In order to produce the streamers, multiple laser-induced bubbles were generated simultaneously over a line by focusing a high-power Nd-YAG laser pulse (*Spectra Physics Quanta-Ray*, $\lambda = 532$ nm) along the center of an acoustic chamber containing phosphoric acid, by means of the optical arrangement detailed in Figure 1(a). The bubble seeding takes place while the chamber was driven with high-intensity ultrasound, favoring the nucleation of the cavities. A detailed description of the experimental setup can be found in Ref. [6].

The acoustic resonator was made from an optical glass cubical cuvette (*Hellma*) with 5 cm of inner length and a wall thickness of 2.5 mm, and was filled with a phosphoric acid aqueous solution 75% w/w (PA75) saturated with air at ambient pressure.

The driving system was built from a ring-shaped piezoceramic transducer (PZT; 30.5 mm OD, 11 mm ID and 5 mm thickness) attached to the bottom wall of the cuvette. The acoustic signal was measured with a smaller PZT disc (MIC; 5 mm in diameter and 2 mm in thickness) mounted on the outer wall of the cuvette (as shown in Fig. 1(b)). The driving frequency was set to 26.1 kHz, which matches one resonant mode of the system with a pressure antinode near the cuvette center. The MIC signal was correlated with the acoustic pressure amplitude following the procedure detailed in Ref. [6]. The liquid temperature was close to 295 K in all the measurements. The average value of the laser pulse power P_L was characterized with a thermopile sensor *Coherent LM10* plugged to a power/energy analyzer *FieldMaster-GS FM 33-0506*. The images of the streamers were captured using two cameras with two different settings: (i) long exposure time (100 ms) photographs were taken with a *Nikon D700* equipped with a 60 mm objective, and (ii) high-speed videos were taken with a *Photron SA5* camera equipped with a long-distance microscope *Infinity K2 Distamax* (Fig. 1(a)). The fast recordings were taken with 35 kfps and an exposure time of 1 µs, which allowed to image details of the bubble seeding and streamer evolution.

Results

Cavitation bubbles were seeded in the phosphoric acid with a random acoustic phase (ϕ_s). In some of the experiments, laser-induced bubbles were produced maintaining the driving voltage fixed at 300 V_{rms} (corresponding to $|P_{Ac}| \simeq 5.85$ bar at the pressure antinode location) to evaluate the effect of the laser pulse power P_L on the streamer development. In the remaining set of measurements, $|P_{Ac}|$ was varied between (1.2 ± 0.1) bar and (8.5 ± 0.1) bar. Here, the laser energy was adjusted to the minimum required for the shot to produce a single bubble for $|P_{Ac}| \sim 1.2$ bar (the minimum value used).

Bubble "lightning" streamers

The laser was directly focused with a relatively small convergence angle, resulting in a double cone as shown in Fig. 2(a). The region of sufficient light energy to seed a bubble in the cuvette therefore corresponded to a an elongated ellipsoid stretched in beam direction, with a maximum on the convergence point. As a consequence of the Gaussian profile of the laser beam, the bubble seeding occurred mainly along a line on the beam axis. The line length ranged from 1 mm to 40 mm, depending strongly on P_L and weakly on $|P_{Ac}|$. After the inception of the

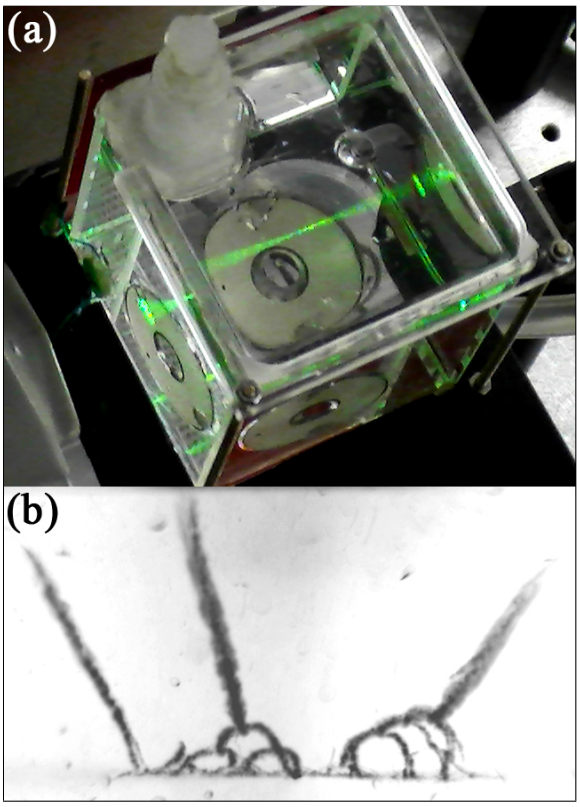

Figure 2: Inception of a bubble chain over a line. (a) Photograph of the green laser focused beam. (b) Bubble "lightning" streamer photographed orthogonal to the laser beam with a *Nikon D700* camera and an exposure time of 100 ms.

linear multi-bubble structure, the acoustic forces generated streamers following very peculiar paths as shown in Fig. 2(b). The resemblance between this phenomenon and the "Lichtenberg figures" of electric discharges motivated us to refer to these kind of streamers as "bubble lightnings". Driven by repulsive primary Bjerknes forces the bubbles stream away from the anti-nodal region until they reach a position where $\vec{F}_{Bj}$ takes a null value [2, 3] (close to the border of the picture frame). In that point the acoustic pressure intensity is low and usually the bubbles dissolve into the liquid after times of the order of a second. The image further shows evidence of strong bubble-bubble interaction by $\vec{F}^{(2)}_{Bj}$, seen by the junction of the paths.

In principle both $|P_{Ac}|$ and P_L affect the size, the number and the distribution of the seeded bubbles along the line. Figure 3 illustrates the first case. For low values of $|P_{Ac}|$ just one or a few bubbles are seeded in the liquid. Since the region with positive (repulsive) $\vec{F}_{Bj}$ is small at small $|P_{Ac}|$, the seeded bubbles barely shift away from the pressure antinode. When $|P_{Ac}|$ is increased (at fixed P_L), more bubbles are seeded, and the bubble cluster becomes longer. The bubbles are expelled from the cuvette center more violently, and the lines drawn by the bubbles in the pictures get thicker, independently of the specific position on the line. An increase in the bubble interaction is also observed, which produces more ramifications in the streamer pattern. Something similar happens when P_L is increased. However, as a distinctive characteristic, a lack of homogeneity in the bubble numbers and sizes emerges. As shown in Fig. 4, the bubbles generated near the laser focus are considerably bigger, and consequently the streamers originating in the middle of the cluster look thicker and darker. A deeper analysis on the origin of this inhomogeneity is given in the next subsection.

Streamer details from high-speed videos

The selection of frames presented in Fig. 5 illustrates the formation and the temporal evolution of the "bubble lightnings" described above. Initially, while the bubbles are small, the attractive interaction forces between them (i.e. secondary Bjerknes forces) are dominant over the primary Bjerknes forces that push them upwards. This happens mainly due to the tight packing of the cavities composing the cluster. The bubbles stay near the line where they have been seeded and start grouping into small clusters immediately after the inception. After this initial clustering some bubbles coalesce and form bigger bubbles. The big bubbles are more sensible to the primary Bjerknes force, and consequently they are driven upwards from the seeding region. All streamer traces are composed of such big "leading" bubbles (typically $R_{max} \sim 200$ µm) that are followed by a tail of up to hundreds of tiny bubbles. The trail bubbles have maximum radii ranging from 40 µm down to values below the pixel resolution of 10 µm. Many tiny bubbles can be still visualized since they produce slightly darker pixels than the intensity of the background pixels. Repeated merging processes of leader bubbles can happen, producing the branched pattern of streamer paths. For instance in the seventh frame of Fig. 5 the balance between the two Bjerknes forces starts to shift again. As the bubbles slowly drift away from the antinode, the magnitude of both $|P_{Ac}|$ and $\vec{F}_{Bj}$ decay [3]. At the same time, the initial growth in the size of the leading bubbles produces stronger bubble-bubble interactions ($\vec{F}^{(2)}_{Bj}$) resulting in a dominant mutual attraction of neighboured leader bubbles. This finally provokes a change in their movement direction and eventually leads to mutual collision and merging as shown in the eleventh frame of Fig. 5. As discussed before in the text, an increase of both P_L or $|P_{Ac}|$ results in a broadening of the streamers. The high-speed recordings revealed that the origin of this broadening relies on the tail of micro-bubbles (and maybe nano-bubbles) produced by the progressive fragmentation of the bigger bubbles. First, a break up of the seeded bubbles forming the initial clusters, and later the constant rupture of the leading bubbles in the streamers contribute to the tail bubble population. The highly un-

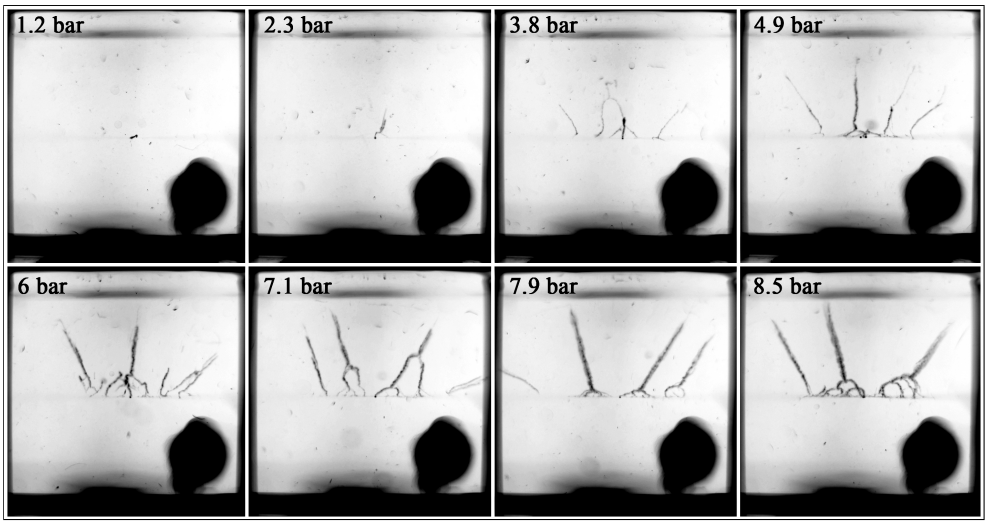

Figure 3: Bubble "lightnings" generated with $P_L \simeq 12$ mW and $|P_{Ac}|$ ranging from $|P_{Ac}| \simeq 1.2$ bar to $|P_{Ac}| \simeq 8.5$ bar.

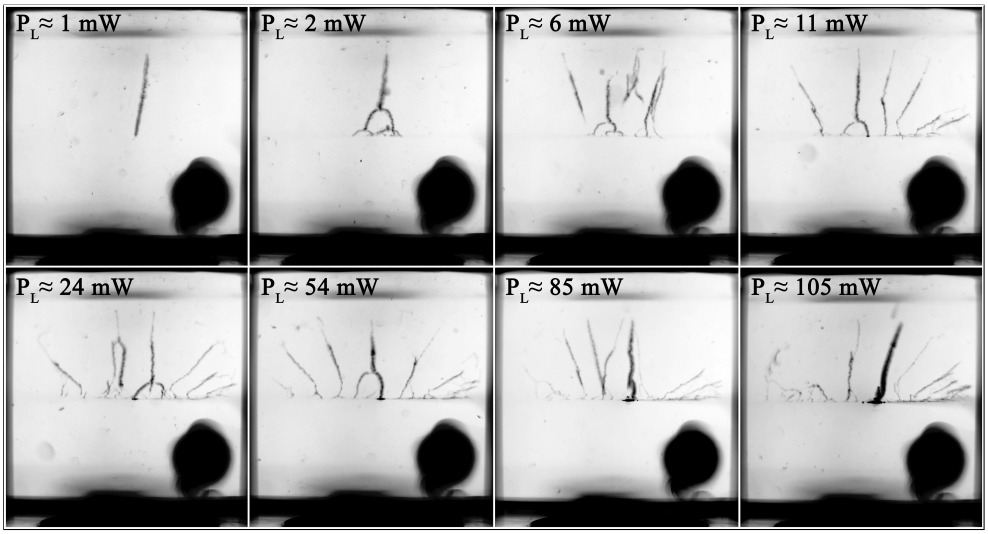

Figure 4: Streamers generated with a fixed value of $|P_{Ac}| \simeq 6$ bar and P_L varying from $P_L \simeq 1$ mW to $P_L \simeq 105$ mW.

stable (non-spherical) shape of the bubbles in both cases can be observed in Fig. 5.

Numerical Simulations

The pressure field of the cuvette was calculated in 3D using the multiphysics software COMSOL (*COMSOL AB, Sweden*). A vertical 2D slice of the central pressure field was extracted and imported into MATLAB (*MathWorks, USA*) where the bubble dynamics were calculated in 2D employing a particle model [5]. This approach simulates the paths of individual bubbles based on a force balance including primary and secondary Bjerknes forces and a drag force. Here, 30 bubbles of a rest radius of $R_0 = 5\mu m$ were randomly seeded in a thin rectangular space representing the laser focal region. The bubble volume oscillations were calculated with the Keller-Miksis equation supposing spherical bubbles. To alleviate numerical divergence problems for approaching bubbles, the model uses higher order terms in the coupling [7], accounting for the strong interaction between bubbles at close spacing and the high pressure inside the cuvette (up to 8 bar). In that context, $\vec{F}_{Bj}^{(2)}$ becomes greater than $\vec{F}_{Bj}$ at close distances of about 0.2 mm [4, 5] and can lead to coalescence. Therefore a coalescence condition is used whereby two bubbles are forced to coalesce when the distance between them is smaller than some critical distance d_{min}, here set to 0.5 mm. Note that this value is somehow larger than those reported in previous work [7, 8] due to the presence of several close neighbour bubbles, together with the strong pressure field. The resulting bubble after merging has the combined volume of the previous two bubbles and conserves their momentum. In Fig. 6, time trace plots of the bubble movement in the pressure field are shown. Similar to the observations in the experiments, the bubbles begin to coalesce into bigger bubbles after some milliseconds, and continue to move upwards, away from the antinode. As they move away, these bigger bubbles still approach each other and eventually coalesce with other bubble clusters, resembling the experiment. Additionally, the times needed for the bubbles to reach the region with null primary Bjerknes force in the simulations have an excellent agreement with the times observed in the experiments for similar cases.

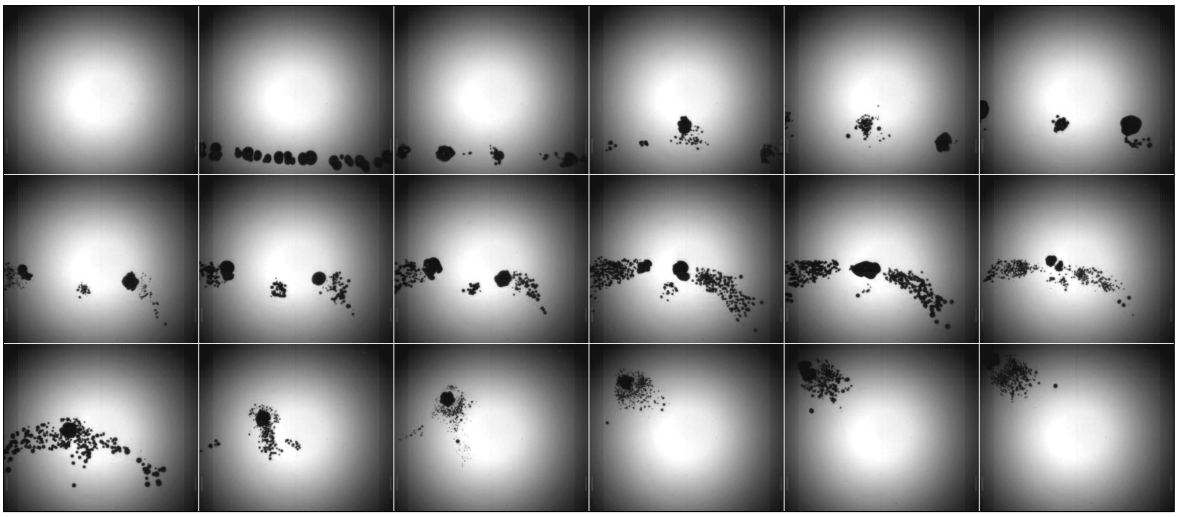

Figure 5: Detail of the streamers formation process for a typical case produced with $P_L \simeq 12$ mW and $|P_{Ac}| \simeq 6$ bar. The frame size is 4.56 mm width by 4.15 mm height, exposure time 1 µs (frames left to right, top to bottom).

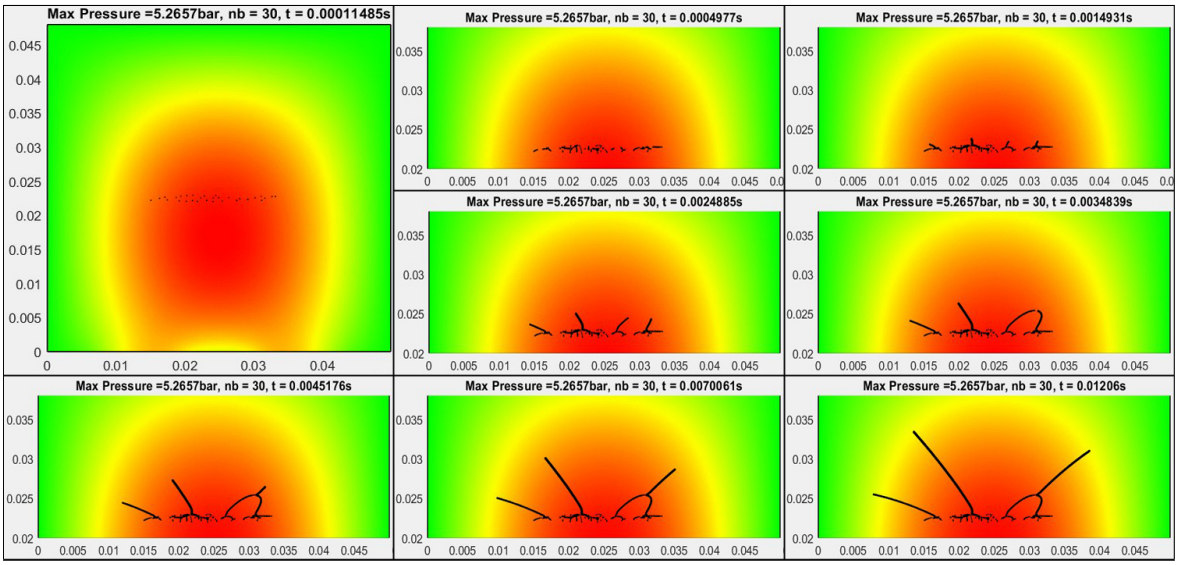

Figure 6: Numerical simulations of "bubble lightnings": 30 bubbles of $R_0 = 5\mu m$ were seeded along a line. The acoustic pressure amplitude at the antinode was set to $|P_{Ac}| = 5.26$ bar (red color), the sound-soft walls have zero pressure (green).

Conclusions

It is remarkable that the experimental streamer paths of the multibubble clusters (leading bubble and trail) behave in average very similarly to the single bubble case treated in the numerical model. This is further indication that dense bubble clusters can be treated as individual bubbles in this context, a phenomenon also noted before in Ref. [9]. Neglecting the dynamic nature of the cluster elements (consisting of permanent interaction of the large and the smaller bubbles, potential splitting and merging) one can assign effective Bjerknes forces to the ensemble and reproduce their motion. In that direction, this kind of controlled experiments can be very useful to train numerical models in order to reproduce the complex dynamic behaviour of bubble clusters in different scenarios. For this it would be critical to find a proper coalescence ratio for modelling the merging and splitting of the bubbles and reproduce the high permanence of the multiple bubbles observed in the experiments.

Acknowledgement: D.S. and R.M. acknowledge funding from the European Union's Horizon 2020 research and innovation program under the Marie Skłodowska-Curie grant agreement No 721290. This publication reflects only the author's view exempting the Community from any liability. Project website: http://cosmic-etn.eu/.

References

[1] R. Mettin, in: T. Kurz *et al* (eds.): *Oscillations, Waves and Interactions* (Universitätsverlag Göttingen, 2007), pp. 171-198.
[2] I. Akhatov *et al*, Phys. Rev. E 55, (1997) 3747-3750.
[3] J. M. Rosselló *et al*, Ultra. Sonochem. 22, (2015) 59-69.
[4] R. Mettin *et al*, Phys. Rev. E 56 (3), (1997) 2924-2931.
[5] R. Mettin *et al*, Ultrason. Sonochem. 6, (1999) 25-29.
[6] J. M. Rosselló *et al*, Phys. Fluids 30 (2018) 122004.
[7] V. Pandey, Phys. Rev. E 99, (2019) 042209.
[8] J. Jiao *et al*, Ultrasonics 58, 35 (2015).
[9] D. Krefting, dissertation, Georg-August-University Göttingen, 2003.